European Polymer Journal 48 (2012) 532–540

Contents lists available at SciVerse ScienceDirect

European Polymer Journal

journal homepage: www.elsevier.com/locate/europolj

Synthesis and photovoltaic property of polymer semiconductor with phthalimide derivative as a promising electron withdrawing material

Jang Yong Lee, Seung Min Lee, Kwan Wook Song, Doo Kyung Moon *

Department of Materials Chemistry and Engineering, Konkuk University, 1 Hwayang-dong, Gwangjin-gu, Seoul 143-701, Republic of Korea

ARTICLE INFO

Article history:
Received 15 September 2011
Received in revised form 2 November 2011
Accepted 6 December 2011
Available online 14 December 2011

Keywords:
Photovoltaic materials
Phthalimide
Conjugated polymers
Donor materials

ABSTRACT

Donor–acceptor type (DA-type) polymeric photovoltaic material with a dicarboxylic imide-substituted benzene (phthalimide) derivative as electron-withdrawing units, poly[4,4′-didodecyl-2,2′-bithiophene-co-5,5′-(3,6-bis(thieno-2-yl)-*N*-octyl-phthalimide] (PDBTTPT), was synthesized by a Stille coupling reaction. It had an optical band gap of 1.96 V and a relatively low HOMO energy level of −5.34 eV in spite of it being a thiophene-based polymer. Photovoltaic devices with PDBTTPT/$PC_{71}BM$ active layers were fabricated under a variety of conditions for optimizing device performance. PDBTTPT exhibited the best power conversion efficiency (PCE) of 1.5% in the device where 80 wt.% of the $PC_{71}BM$ was contained in the active layer (PDBTTPT:$PC_{71}BM$ = 1:4, w/w) and which was pre-annealed at 120 °C for 10 min. In addition, a device which was pre-annealed at 140 °C for 10 min and a device which was post-annealed at 120 °C for 10 min showed analogous PCE values of 1.5% as well, although small differences were exhibited between various parameters, such as V_{OC}, J_{SC}, and FF.

1. Introduction

Organic photovoltaic devices based on polymer semiconductors are clean and efficient electronic devices that directly generate usable electricity by reactions between photons from solar irradiation and semiconductor materials in their active layers. In this respect, in order to develop a high performance organic photovoltaic device, the key technology is the design and synthesis of polymer semiconductor materials. Photovoltaic polymer materials have gained considerable attention for two decades due to their various advantages, such as low-cost, flexibility, eco-friendly use, etc. Recently, developments of several high-performance organic photovoltaic materials [1–9] and researches for photochemical stability of π-conjugated polymers have increased the potential for organic photovoltaic applications [10,11]. Moreover, fabrication technologies of flexible and large area devices, such as ink-jet printing and roll-to-roll through solution processing [12–16], have increased the practical potential of these materials towards next generation energy converting devices.

Since organic photovoltaic devices had been investigated, a variety of strategies have been used for developing high efficiency polymeric photovoltaic materials [17–21]. Among them, the synthesis of copolymers that alternate electron donating materials with electron withdrawing materials in polymer backbones has been regarded as the most efficient strategy for synthesizing photovoltaic materials since the polymer band gap was effectively controlled by the intra-chain charge transfer [22,23]. In order to develop outstanding donor–acceptor (DA) type copolymers, the most important consideration is the choice of electron-donating and electron-withdrawing materials that had various favorable properties, such as good solubility, appropriate energy level, structural planarity, etc.

In this respect, phthalimide is a promising electron-withdrawing material for organic photovoltaics. The solubility and the energy levels of phthalimide can be easily controlled by introducing various functional groups at its

* Corresponding author. Tel.: +82 2 450 3498; fax: +82 2 444 0765.
E-mail address: dkmoon@konkuk.ac.kr (D.K. Moon).

0014-3057/$ - see front matter © 2011 Elsevier Ltd. All rights reserved.
doi:10.1016/j.eurpolymj.2011.12.006

nitrogen site. Moreover, the highest occupied molecular orbital (HOMO) energy level of a polymer with phthalimide in its polymer backbone could also be easily lowered because of the low HOMO energy level of phthalimide, which leads to improved open circuit voltage (V_{OC}) values of final devices. Nevertheless, there are almost no investigations concerning polymeric materials with phthalimide for OPVs, except for a few studies [24,25].

In this study, a DA-type polymer semiconductor that had a phthalimide as an electron-withdrawing moiety, PDBTTPT, was synthesized through a Stille coupling reaction for organic photovoltaic materials. Bulk heterojunction-type devices with 1-(3-methoxycarbonyl)propyl-1-phenyl-6,6-C-71 ($PC_{71}BM$) as acceptors were fabricated in order to investigate the photovoltaic properties of PDBTTPT. Additionally, in order to optimize device performance, photovoltaic devices were fabricated under a variety of conditions, according to different weight ratios between PDBTTPT and $PC_{71}BM$ or various annealing temperatures and times.

2. Experimental section

2.1. Materials

All reagents were purchased from Aldrich and were used without further purification. 4,4′-Didodecyl-5,5′-trimethylstannyl-2,2′-bithiophene [26] were prepared as described in the literature.

2.1.1. 3,6-Dibromophthalic anhydride (**1**)

A mixture of phthalic anhydride (5.9 g, 40 mmol), oleum (20% free SO_3, 75 ml), bromine (13.4 g, 84 mmol) and silver sulfate (25 g, 80.2 mmol) was stirred at 70 °C for 24 h. After cooling to room temperature, precipitations were filtered off and washed by dichloromethane. The solution was washed with water and extracted with chloroform. The organic layer was concentrated via rotary evaporation to a brown solid. This brown solid was recrystallized twice from acetic acid to provide colorless crystals (1.4 g, 4.6 mmol). ^{1}H NMR (400 MHz; $CDCl_3$; Me_4Si): 7.85 (s, 2H). ^{13}C NMR (100 MHz; $CDCl_3$; Me_4Si): 159.15, 141.55, 131.10, 120.16.

2.1.2. N-Octyl-3,6-dibromophthalimide (**2**)

Compound **1** (1.4 g, 4.6 mmol) was dissolved in glacial acetic acid (25 ml) followed by dropwise of octyl amine (0.78 g, 6.0 mmol). The mixture was refluxed under nitrogen for 2 h. After most of the acetic acid was removed under reduced pressure, the crude product was purified using column chromatography using dichloromethane/hexane (1:3, v/v) as the eluent. Colorless crystals were obtained after recrystallization from hexanes (1.6 g, 3.9 mmol). ^{1}H NMR (400 MHz; $CDCl_3$; Me_4Si): 7.62 (d, 2H), 3.66 (d, 2H), 1.65 (m, 2H), 1.37–1.24 (m, 10H), 0.87 (t, 3H). ^{13}C NMR (100 MHz; $CDCl_3$; Me_4Si): 165.05, 139.68, 131.51, 117.69, 38.05, 31.33, 28.97 (2C), 28.05, 26.88, 22.87, 13.98.

2.1.3. 3,6-Bis(thieno-2-yl)-N-octyl-phthalimide (**3**)

Compound **2** (1.6 g, 3.9 mmol), 2-tributylstannylthiophene (3.7 g, 9.8 mmol) and $Pd(PPh_3)_2Cl_2$ (5 mol%) were dissolved in a mixture of THF (40 ml). The mixture was refluxed for 24 h. After cooling to room temperature, the organic layer was dried with Na_2SO_4 and was concentrated via rotary evaporation. The product was purified using column chromatography using dichloromethane/hexane (1:3, v/v) as the eluent. The product was obtained as bright yellow solid (1.15 g, 2.7 mmol). ^{1}H NMR (400 MHz; $CDCl_3$; Me_4Si): 7.77 (d, 2H), 7.76 (s, 2H), 7.47 (d, 2H), 7.17 (t, 2H), 3.66 (d, 2H), 1.65 (m, 2H), 1.37–1.24 (m, 10H), 0.87 (t, 3H). ^{13}C NMR (100 MHz; $CDCl_3$; Me_4Si): δ 167.02, 137.24, 135.87, 132.31, 130.00, 127.95, 127.72, 127.54, 38.27, 31.64, 29.05 (2C), 28.18, 26.96, 22.96, 14.04.

2.1.4. 5,5′-Dibromo-3,6-bis(thieno-2-yl)-N-octyl-phthalimide (**4**)

Compound **3** (1.15 g, 2.7 mmol) were dissolved to mixture of chloroform/acetic acid (1:1, v/v) at room temperature. NBS (1.0 g, 5.9 mmol) was added to the mixture. After 24 h, the mixture was poured to water and organic layer was extracted with chloroform. The organic layer was dried with Na_2SO_4 and was concentrated via rotary evaporation. The product was purified using column chromatography using dichloromethane/hexane (1:3, v/v) as the eluent. The product was obtained as bright yellow solid (0.87 g, 1.5 mmol). ^{1}H NMR (400 MHz; $CDCl_3$; Me_4Si): 7.70 (s, 2H), 7.52 (d, 2H), 7.12 (d, 2H), 3.66 (d, 2H), 1.66 (m, 2H), 1.33–1.20 (m, 10H), 0.86 (t, 3H). ^{13}C NMR (100 MHz; $CDCl_3$; Me_4Si): 167.27, 138.48, 135.27, 131.43, 130.55, 130.38, 127.88, 115.10, 38.35, 31.79, 29.16 (2C), 28.46, 26.97, 22.64, 14.12.

2.1.5. PDBTTPT

4,4′-Didodecyl-5,5′-trimethylstannyl-2,2′-bithiophene (0.41 g, 0.5 mmol), compound **4** (0.30 g, 0.5 mmol) and $Pd(PPh_3)_2Cl_2$ (1.5 mol%) were dissolved in THF/DMF (1/1, v/v). The solution was refluxed for 48 h with vigorous stirring in nitrogen atmosphere, and then the excess amount of bromothiophene and 2-tributylstannylthiophene were added and stirring continued for 3 h, respectively. The whole mixture was poured into methanol. The precipitate was filtered off, purified with methanol, acetone and hexane in a Soxhlet apparatus for 24 h, respectively. The chloroform soluble fraction was recovered and dried under a reduced pressure at 80 °C. The product was obtained as dark red powder (0.13 g, 27%). ^{1}H NMR (400 MHz; $CDCl_3$; Me_4Si): 7.86 (d, 2H), 7.80 (s, 2H), 7.19 (d, 2H), 7.05 (s, 2H), 3.70 (t, 2H), 2.81 (t, 4H), 1.71 (m, 4H), 1.61 (m, 2H),1.5 – 1.2 (br, 8H), 0.87 (t, 3H). Elem. Anal. for $C_{56}H_{75}N_1S_4O_2$: C, 72.91; H, 8.19; N, 1.52; S, 13.91; O, 3.47. Found: C, 72.84; H, 8.22; N, 1.53; S, 13.99; O, 3.42.

2.2. Instruments and characterization

All of the reagents and chemicals were purchased from Aldrich and used as received unless otherwise specified. The ^{1}H NMR (400 MHz) spectra were recorded using a Brüker AMX400 spectrometer in $CDCl_3$, and the chemical shifts were recorded in units of ppm with TMS as the internal standard. The elemental analyses were measured with EA1112 using a CE Instrument. The absorption spectra were recorded using an Agilent 8453 UV–vis spectroscopy

system. The solutions that were used for the UV–vis spectroscopy measurements were dissolved in chloroform at a concentration of 10 μg/ml. The films were drop-coated from the chloroform solution onto a quartz substrate. All of the GPC analyses were carried out using THF as the eluent and a polystyrene standard as the reference. The DSC and the TGA measurements were performed using a NETZSCH DSC 200 F3 and a NETZSCH TG 209 F3, respectively. The cyclic voltammetric waves were produced using a Zahner IM6eX electrochemical workstation with a 0.1 M acetonitrile (substituted with nitrogen for 20 min) solution containing tetrabutyl ammonium hexafluorophosphate (Bu_4NPF_6) as the electrolyte at a constant scan rate of 50 mV/s. ITO, a Pt wire, and silver/silver chloride [Ag in 0.1 M KCl] were used as the working, counter, and reference electrodes, respectively. The electrochemical potential was calibrated against Fc/Fc^+. The HOMO levels of the polymers were determined using the oxidation onset value. Onset potentials are values obtained from the intersection of the two tangents drawn at the rising current and the baseline changing current of the CV curves. The LUMO levels were calculated from the differences between the HOMO energy levels and the optical band-gaps, which were determined using the UV–vis absorption onset values in the films.

The current–voltage (I–V) curves of the photovoltaic devices were measured using a computer-controlled Keithley 2400 source measurement unit (SMU) that was equipped with a Peccell solar simulator under an illumination of AM 1.5G (100 mW/cm^2). Thicknesses of the thin films were measured using a KLA Tencor Alpha-step 500 surface profilometer with an accuracy of 1 nm. Topographic images of the active layers were obtained through atomic force microscopy (AFM) in tapping mode under ambient conditions using a XE-100 instrument.

2.3. Fabrication and characterization of polymer solar cells

All of the bulk-heterojunction PV cells were prepared using the following device fabrication procedure. The glass/indium tin oxide (ITO) substrates [Sanyo, Japan (10 Ω/γ)] were sequentially lithographically patterned, cleaned with detergent, and ultrasonicated in deionized water, acetone, and isopropyl alcohol. Then the substrates were dried on a hot-plate at 120 °C for 10 min and treated with oxygen plasma for 10 min in order to improve the contact angle just before the film coating process. Poly(3,4-ethylene-dioxythiophene): poly(styrene-sulfonate) (PEDOT:PSS, Baytron P 4083 Bayer AG) was passed through a 0.45 μm filter before being deposited onto ITO at a thickness of ca. 32 nm by spin-coating at 4000 rpm in air and then it was dried at 120 °C for 20 min inside a glove box. Composite solutions with PDBTTPT and $PC_{71}BM$ were prepared using o-dichlorobenzene (o-DCB). The concentration was controlled adequately in the 0.5 wt.% range, and the solutions were then filtered through a 0.45 μm PTFE filter and then spin-coated (500–1700 rpm, 30 s) on top of the PEDOT:PSS layer. The device fabrication was completed by depositing thin layers of BaF_2 (1 nm), Ba (2 nm), and Al (200 nm) at pressures of less than 10^{-6} torr. The active area of the device was 4.0 mm^2. Finally, the cell was encapsulated using UV-curing glue (Nagase, Japan). In this study, all of the devices were fabricated with the following structure: ITO glass/PEDOT:PSS/polymer:PCBM/BaF_2/Ba/Al/ encapsulation glass.

The illumination intensity was calibrated using a standard a Si photodiode detector that was equipped with a KG-5filter. The output photocurrent was adjusted to match the photocurrent of the Si reference cell in order to obtain a power density of 100 mW/cm^2. After the encapsulation, all of the devices were operated under an ambient atmosphere at 25 °C.

3. Results and discussion

3.1. Material synthesis

The synthesis process for the monomers and PDBTTPT is shown in Scheme 1. Since thiophene has a good electron donating and charge transporting property, dodecylbithiophene was adopted as the electron-donating unit. Long alkyl chains (dodecyl chains) were introduced in the bithiophene unit to improve solubility. In addition, in order to minimize the steric hindrance between the dodecyl chains, dodecylbithiophene was synthesized in a tail-to-tail formation. Thiophene spacers that neighbored the phthalimide molecule were introduced into the polymer backbone to decrease the band gap by enlarging the π-conjugation length and to diminish the steric hindrance between the electron-donating unit and the electron-withdrawing moiety [27].

The number average molecular weight (M_n) and the weight average molecular weight (M_w) of PDBTTPT were 16.7 and 22.2 kg/mol, respectively. The thermal properties of PDBTTPT were investigated using differential scanning calorimetry (DSC) and thermogravimetric analysis (TGA) at a heating rate of 10 K/min. As shown in Fig. 1, the polymers had a glass transition temperature (T_g) of 146 °C and decomposition temperature (T_d) of 387 °C, which indicated that they exhibited good thermal stability, making them applicable for use in polymer solar cells and other optoelectronic devices. Particularly, PDBTTPT indicated a high T_g, which stemmed from its rigid backbone structure and its phthalimide molecules.

3.2. Optical and electrochemical properties

The UV–vis absorption spectra of PDBTTPT in a chloroform solution and in thin solid films are depicted in Fig. 2. A maximum UV–vis absorption peak (λ_{max}) appeared at 457 nm in solution. And the λ_{max} value in the solid film was displayed at 526 nm, and this was red-shifted by approximately 70 nm. In addition, a shoulder peak was shown at around 570 nm. This indicated that PDBTTPT had a good intermolecular interaction property in solid film [28]. However, in spite of its outstanding red-shifted UV–vis absorption property, the UV–vis absorption range of PDBTTPT was not wide in comparison with other DA-type copolymers. It seemed that the electron-withdrawing property of phthalimide was not as strong as typical electron-withdrawing material, 2,1,3-benzothiadiazole.

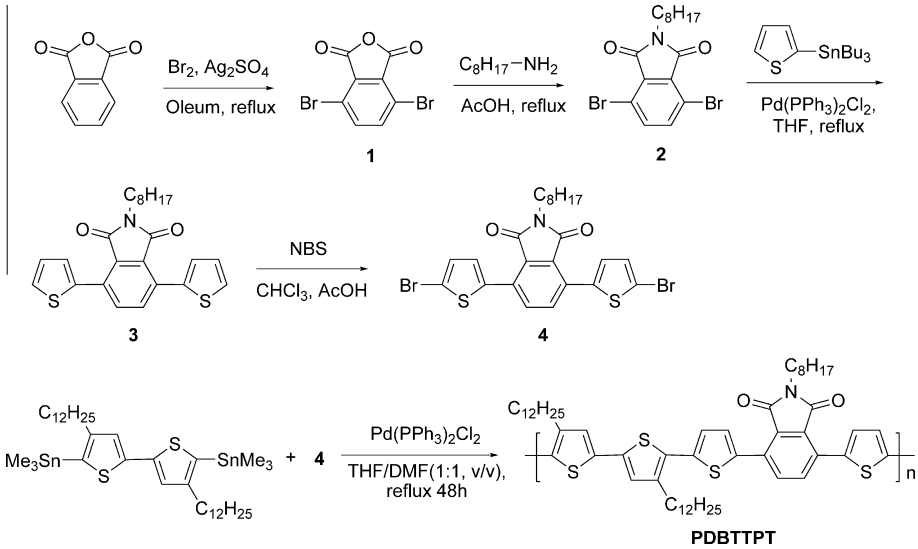

Scheme 1. The synthetic route of PDBTTPT.

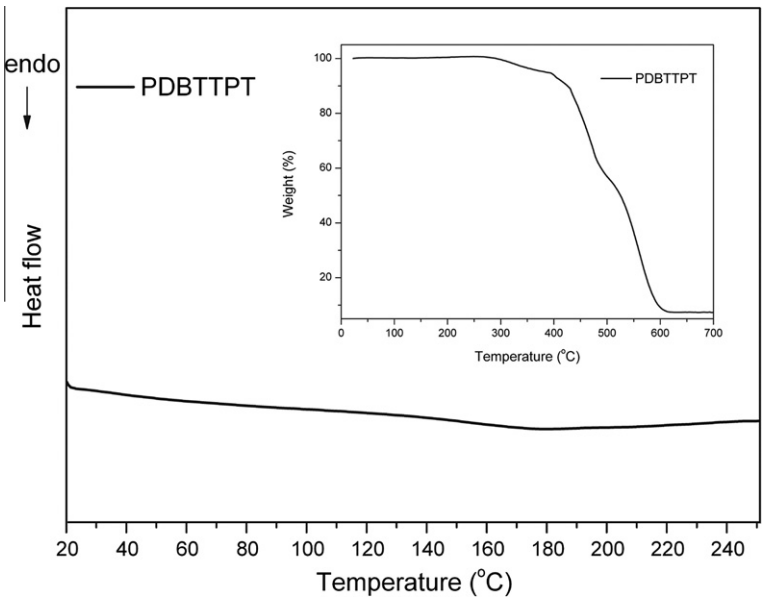

Fig. 1. DSC thermogram of PDBTTPT (inset: TGA curve of PDBTTPT).

Generally, band gap energy of DA-type copolymer is effectively decreased by orbital overlap through charge transfer between electron-donating materials and electron-withdrawing materials. Therefore, in DA-type polymer backbones, the stronger electron-withdrawing property of electron-deficient material was, the narrower the band gap became [29]. However, as shown in Fig. 3, according to a theoretical study, the electron affinity of phthalimide was weaker than that of 2,1,3-benzothiadiazole, which could lead to inefficient charge transfer in intramolecular polymer chains. Nevertheless, as mentioned above, when considering that the HOMO energy level of the polymer was formed by orbital overlap between the HOMO energy levels of the electron-donating material and electron withdrawing material, the low HOMO energy level of phthalimide could have an influence on lowering the HOMO energy level of PDBTTPT, which was one of the most important requirements for oxidative stability and high V_{OC} of photovoltaic polymer materials. The optical band gap (E_g^{op}) of PDBTTPT, which was calculated from the band edge of the UV–vis absorption spectra in the film, was 1.96 eV.

The electrochemical behavior of the copolymers was investigated using cyclic voltammetry (CV). The supporting electrolyte was tetrabutyl ammonium hexafluorophosphate (Bu_4NPF_6) in acetonitrile (0.1 M), and the scan rate

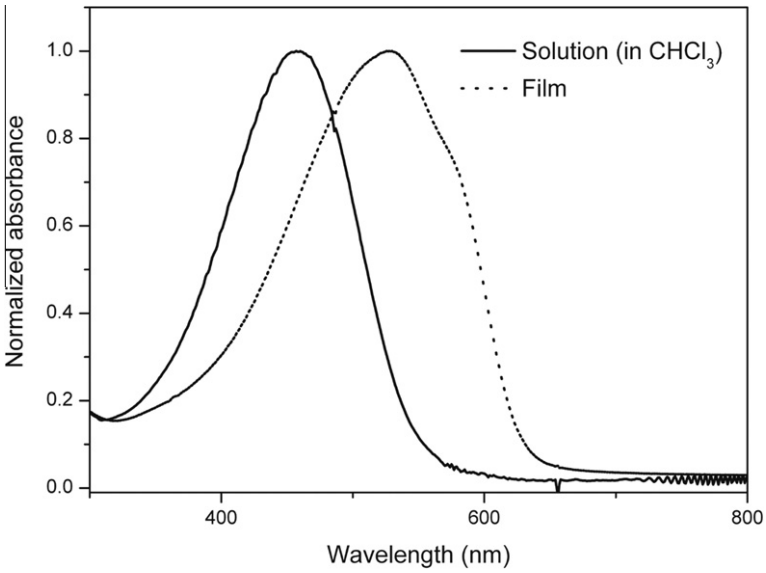

Fig. 2. UV–vis absorption spectra of PDBTTPT.

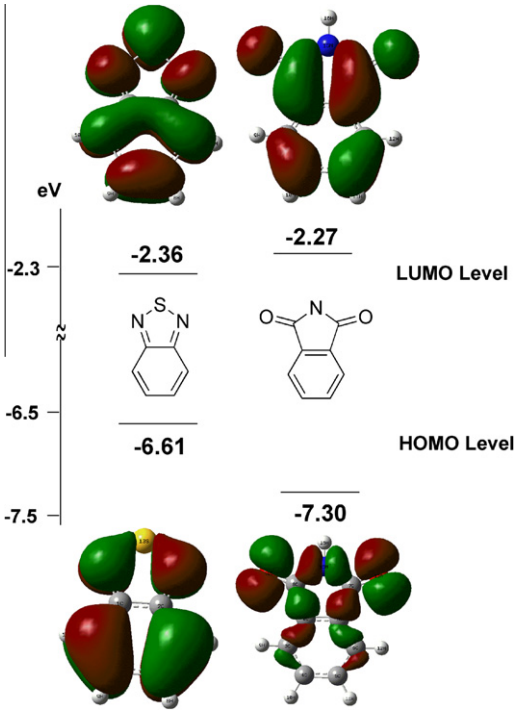

Fig. 3. Comparison of theoretical HOMO and LUMO energy levels between 2,1,3-benzothiadiazole and phthalimide.

was 50 mV/s. The ITO glass and Pt plates were used as the working and counter electrodes, respectively, and silver/silver chloride (Ag in 0.1 M KCl) was used as the reference electrode. All of other measurements were calibrated using the ferrocene value of −4.8 eV as the standard. The HOMO levels of the polymers were determined using the oxidation onset value. The lowest unoccupied molecular orbital (LUMO) levels were calculated from the differences between the HOMO energy levels and the optical band-gaps, which were determined using the UV–vis absorption onset values in the films.

Fig. 4 shows the cyclic voltammogram of the PDBTTPT. The HOMO level of this polymer was −5.34 eV and the LUMO level was −3.36 eV. As expected and mentioned above, PDBTTPT exhibited a low HOMO energy level. It should be noted that the HOMO energy level of PDBTTPT was relatively low in comparison with other photovoltaic copolymers based on thiophene derivatives [30]. This originated from the low HOMO energy level of phthalimide. Considering that the V_{OC} value was determined by the difference between the HOMO level of the donor polymer and the LUMO level of the acceptor, it was expected that PDBTTPT would exhibit high V_{OC} values in the final device. The electrochemical band gap (E_g^{ec}) of PDBTTPT was 2.13 eV, and this was determined by the difference between the HOMO and the LUMO energy levels, which were calculated from oxidation and reduction onsets, respectively. A little difference between E_g^{op} and E_g^{ec} was observed. This was because free ions were created in the electrochemical experiment rather than a neutral excited state [31]. The optical and electrochemical properties of the polymers are summarized in Table 1.

3.3. Morphology analysis

The topography images of the PDBTTPT/$PC_{71}BM$ blend films were obtained using AFM on non-contact mode. The topography images showed that detailed p, n-channels appeared as the $PC_{71}BM$ weight ratio increased in Fig. 5(a–c). In addition, aggregated large $PC_{71}BM$ domains were not observed with increases of the $PC_{71}BM$ weight ratio. Hereby, 20 wt.% PDBTTPT and 80 wt.% $PC_{71}BM$ (1/4, w/w) was identified as the most efficient blend ratio between PDBTTPT and $PC_{71}BM$.

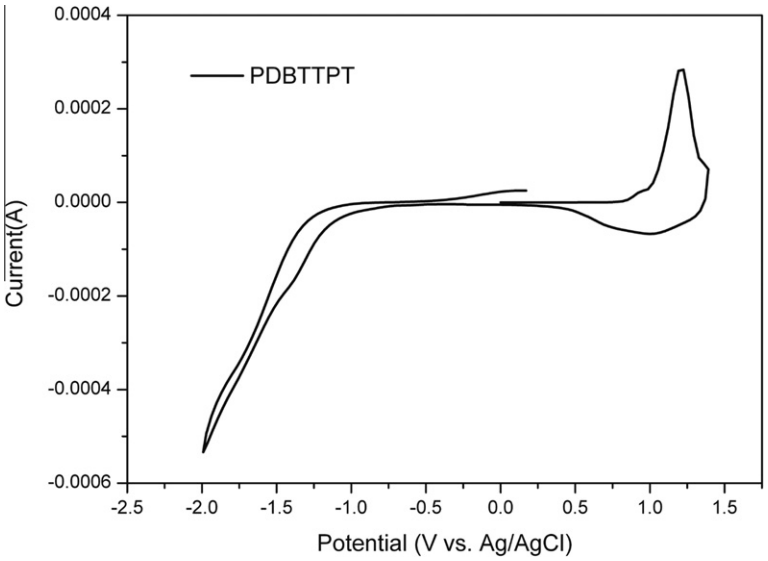

Fig. 4. Cyclic voltammograms of thin film recorded in 0.1 M Bu_4NPF_6/acetonitrile at a scan rate of 50 mV/s.

Table 1
Summary of photovoltaic characteristics of devices.

Active layer		Weight ratio (P:A, w/w)	Annealing (°C, min)	V_{OC} (V)	J_{SC} (mA/cm^2)	FF (%)	PCE (%)
Polymer (P)	Acceptor (A)						
PDBTTPT	$PC_{71}BM$	1:2	(120, 10)[a]	0.85	4.7	33.4	1.3
		1:3	(120, 10) [a]	0.83	5.2	32.2	1.4
		1:4	(120, 10) [a]	0.81	5.9	30.0	1.5
PDBTTPT	$PC_{71}BM$	1:4	(100, 20) [a]	0.77	4.2	33.1	1.1
		1:4	(120, 20) [a]	0.77	4.6	36.0	1.3
		1:4	(140, 10) [a]	0.79	5.0	37.6	1.5
		1:4	(120, 10) [b]	0.85	4.4	39.0	1.5

[a] Pre-annealing.
[b] Post-annealing.

Fig. 5(d–f) shows the topography images of PDBTTPT/$PC_{71}BM$ blend films with different annealing conditions. Fig. 5(e and f) shows the morphology images with relatively efficiently developed networks between the PDBTTPT and $PC_{71}BM$, while the PDBTTPT/$PC_{71}BM$ blend film annealed at 100 °C for 20 min did not efficiently form p, n-channels. This would be due to insufficient kinetic activity for achieving better polymer chain ordering between polymer chains, which results from a low annealing temperature and short annealing time [32]. Differences in the active layer morphologies as above could have an influence on the final photovoltaic device performance, especially with respect to the short circuit current density (J_{SC}) and fill factor (FF).

3.4. Photovoltaic characteristics

Bulk heterojunction solar cells using PDBTTPT as donor materials and $PC_{71}BM$ as an acceptor material were fabricated with a structure of ITO/PEDOT:PSS/active layer/BaF_2/Ba/Al. Since $PC_{71}BM$ has a stronger UV–vis absorption property than does $PC_{61}BM$ in the visible region, especially around 500 nm [33], $PC_{71}BM$, was used as the acceptor material in this research. In order to optimize the active layer thickness, polymer/$PC_{71}BM$ blend films were spin-coated under various conditions (500–1700 rpm, 30 s). All the photovoltaic measurements were performed under 100 mW/cm^2 AM 1.5 sun illumination in ambient conditions. In order to optimize device performance, photovoltaic devices were fabricated under different fabricating conditions, including different weight ratios of $PC_{71}BM$ and different annealing conditions.

As shown in Fig. 6(a), in a comparison of devices with different weight ratios of acceptors, the best power conversion efficiency (PCE) of 1.5% was exhibited in the device where 80 wt.% $PC_{71}BM$ was contained in the active layer (PDBTTPT:$PC_{71}BM$ = 1:4, w/w) while the same thermal annealing conditions were used (120 °C, 10 min). Although this device exhibited a somewhat low open circuit voltage (V_{OC}) value of 0.81 V and FF of 30% in comparison with the other two devices, it had a higher value of J_{SC} (5.9 mA/cm^2). This J_{SC} value originated from the UV–vis absorption property of $PC_{71}BM$. As mentioned above, $PC_{71}BM$ absorbed in the UV–vis spectrum at around 500 nm. Fig. 6(b) explained the reason why the J_{SC} value increased as the $PC_{71}BM$ weight ratio increased. As depicted in Fig. 6(b), as the

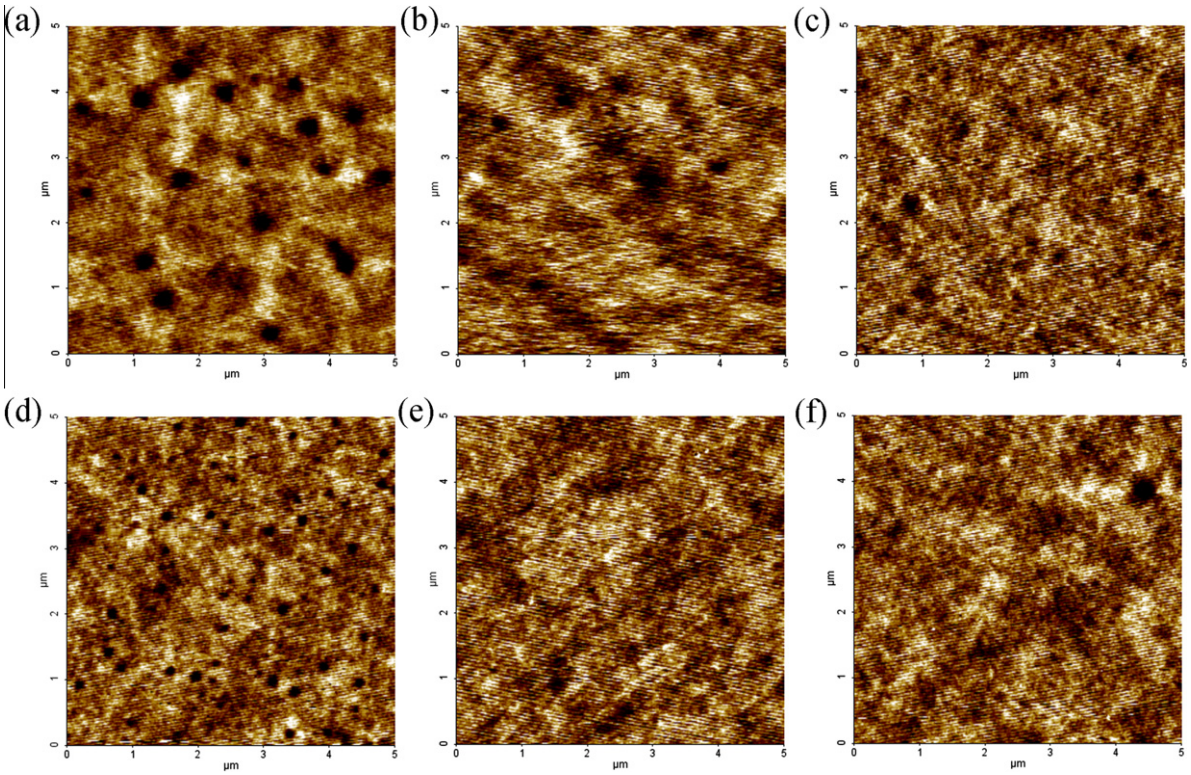

Fig. 5. Topography image obtained non-contact mode AFM on the surface for PDBTTPT/ $PC_{71}BM$ thin films annealed at 120 °C for 10 min (a) (1:2, w/w), (b) (1:3, w/w), (c) (1:4, w/w) and PDBTTPT/$PC_{71}BM$ thin films (1:4, w/w) with different thermal annealing conditions (d) at 100 °C for 20 min (e) at 120 °C for 20 min (f) at 140 °C for 10 min.

$PC_{71}BM$ weight ratio increased, the conversion of photocurrent to electrons was also improved. When comparing the device with 75% $PC_{71}BM$ with 80% $PC_{71}BM$, although the two devices showed analogous maximum external quantum efficiency (EQE) intensities, the latter exhibited more extended EQE spectra toward long wavelengths than the former.

As shown in Fig. 7, the photovoltaic devices with the same $PC_{71}BM$ weight ratio (1:4, w/w) were prepared under various annealing conditions as well. Under pre-annealing conditions, the PCE values of devices increased as the annealing temperature increased. This is due to the increased kinetic activity, which is sufficient for better polymer chain ordering between polymer chains, as mentioned above. The best performance (0.79 V V_{OC}, 5.0 mA/cm^2 J_{SC}, 37.6% FF, and 1.5% PCE) was exhibited in the device where the active layer was annealed at 140 °C for 10 min. Although the device that was pre-annealed at

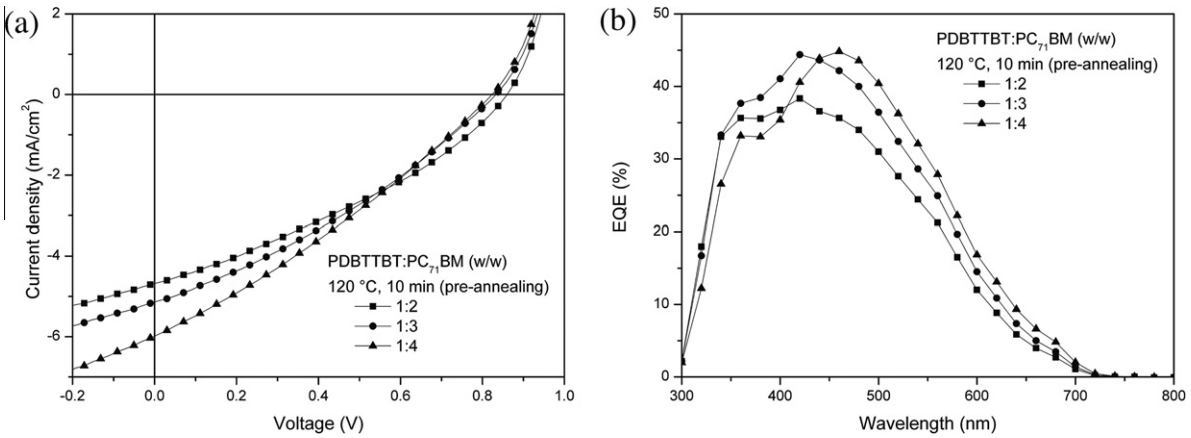

Fig. 6. (a) *J–V* characteristics and (b) EQE spectra of photovoltaic devices as the $PC_{71}BM$ weight ratio increased.

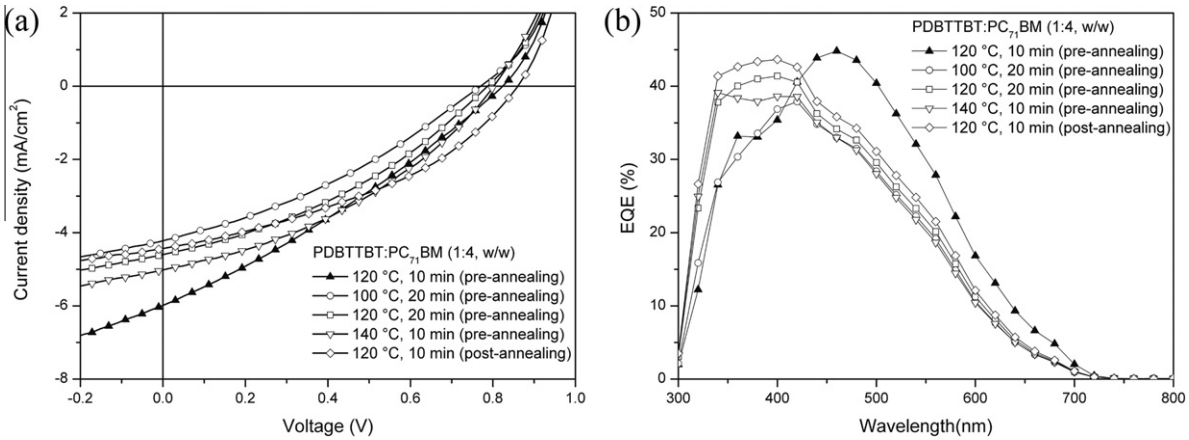

Fig. 7. (a) *J–V* characteristics and (b) EQE spectra of photovoltaic devices with different thermal annealing conditions.

120 °C for 10 min and the device that was pre-annealed at 140 °C for 10 min exhibited the same PCE value (1.5%), there were differences between their other parameters, such as V_{OC}, J_{SC}, and FF. Particularly, the J_{SC} value decreased and the FF increased as the pre-annealing temperature increased. The EQE date explained the reason of the decrease of the J_{SC} value. When pre-annealing at 120 °C for 10 min, the device had an extended absorption spectrum toward a long wavelength region compared with the device that was pre-annealed at 140 °C for 10 min. Considering that the $PC_{71}BM$ absorbed a UV–vis spectrum around 500 nm, the absorption of photons by $PC_{71}BM$ could be disrupted due to the inappropriate annealing conditions, which resulted in a reduced J_{SC} value. The device that was post-annealed at 120 °C for 10 min had the same reason for its reduced J_{SC} value as well. In contrast, the FF increased as the annealing temperature increased, which could be because of the improved morphology property due to the increased kinetic activity of the polymer chains.

As shown in Table 1, the PCE value of PDBTTPT was governed by the J_{SC} value and FF, which was primarily determined by the photon absorption property and device fabrication conditions. If the energy level and band gap of the phthalimide derivative are modified by introducing various functional groups and the device fabrication conditions are optimized, it will be possible to develop high performance photovoltaic materials and devices.

4. Conclusions

PDBTTPT, which is based on phthalimide, was successfully synthesized through the Stille coupling reaction for the OPVs. The best PCE of 1.5% was exhibited in the device with 80 wt.% $PC_{71}BM$ in its active layer (PDBTTPT:$PC_{71}BM$ = 1:4, w/w) and was pre-annealed at 120 °C for 10 min. It was noted that PDBTTPT had a relatively high V_{OC} value in spite of the thiophene-based polymer material. Although PDBTTPT did not exhibit a very high PCE value, the development of various polymer materials with improved photovoltaic performance by modification of phthalimide moieties is possible.

Acknowledgments

This research was supported by a Grant from the Fundamental R&D Program for Core Technology of Materials funded by the Ministry of Knowledge Economy, Republic of Korea and the National Research Foundation of Korea Grant funded by the Korean Government (MEST) (NRF-2009-C1AAA001-2009-0093526).

References

[1] Huo L, Zhang S, Guo X, Xu F, Li Y, Hou J. Replacing alkoxy groups with alkylthienyl groups: a feasible approach to improve the properties of photovoltaic polymers. Angew Chem Int Ed 2011;50:9697–702.
[2] Bronstein H, Chen Z, Ashraf RS, Zhang W, Du J, Durrant JR, et al. Thieno[3,2-b]thiophene-Diketopyrrolopyrrole-containing polymers for high-performance organic field-effect transistors and organic photovoltaic devices. J Am Chem Soc 2011;133:3272–5.
[3] Ong KH, Lim SL, Tan HS, Wong HK, Li J, Ma Z, et al. A versatile low bandgap polymer for air-stable, high-mobility field-effect transistors and efficient polymer solar cells. Adv Mater 2011;23:1409–13.
[4] Zhao G, He Y, He C, Fan H, Zhao Y, Li Y. Photovoltaic properties of poly-(benzothiadiazole-thiophene-co-bithiophene) as donor in polymer solar cells. Sol Energy Mater Sol Cells 2011;95:704–11.
[5] Hou Q, Xu X, Guo T, Zeng X, Luo S, Yang L. Synthesis and photovoltaic properties of fluorene-based copolymers with narrow band-gap units on the side chain. Eur Polym J 2010;46:2365–71.
[6] Zoombelt AP, Mathijssen SGJ, Turbiez MGR, Wienk MM, Janssen RAJ. Small band gap polymers based on diketopyrrolopyrrole. J Mater Chem 2010;20:2240–6.
[7] Zhang Y, Hau SK, Yip HL, Sun Y, Acton O, Jen AKY. Efficient polymer solar cells based on the copolymers of benzodithiophene and thienopyrroledione. Chem Mater 2010;22:2696–8.
[8] Zhou E, Yamakawa S, Tajima K, Yang C, Hashimoto K. Synthesis and photovoltaic properties of diketopyrrolopyrrole-based donoracceptor copolymers. Chem Mater 2009;21:4055–61.
[9] Zou Y, Gendron D, Neagu-Plesu R, Leclerc M. Synthesis and characterization of new low-bandgap diketopyrrolopyrrole-based copolymers. Macromolecules 2009;42:6361–5.
[10] Manceau M, Bundgaard E, Carlé JE, Hagemann O, Helgesen M, Søndergaard R, et al. Photochemical stability of π-conjugated polymers for polymer solar cells: a rule of thumb. J Mater Chem 2011;21:4132–41.
[11] Jørgensen M, Norrman K, Krebs FC. Stability/degradation of polymer solar cells. Sol Energy Mater Sol Cells 2008;92:686–714.

[12] Krebs FC, Fyenbo J, Tanenbaum DM, Gevorgyan SA, Andriessen R, van Remoortere B, et al. The OE-A OPV demonstrator anno domini 2011. Energy Environ Sci 2011;4:4116–23.
[13] Eom SH, Park H, Mujawar SH, Yoon SC, Kim SS, Na SI, et al. High efficiency polymer solar cells via sequential inkjet-printing of PEDOT:PSS and P3HT:PCBM inks with additives. Org Electron 2010;11:1516–22.
[14] Krebs FC, Gevorgyan SA, Alstrup J. A roll-to-roll process to flexible polymer solar cells: model studies, manufacture and operational stability studies. J Mater Chem 2009;19:5442–51.
[15] Krebs FC. Polymer solar cell modules prepared using roll-to-roll methods: knife-over-edgecoating, slot-die coating and screen printing. Sol Energy Mater Sol Cells 2009;93:465–75.
[16] Niggemann M, Zimmermann B, Haschke J, Glatthaar M, Gombert A. Organic solar cell modules for specific applications—from energy autonomous systems to large area photovoltaics. Thin Solid Films 2008;516:7181–7.
[17] Newman CR, Frisbie CD, da Silva Filho DA, Brédas JL, Ewbank PC, Mann KR. Introduction to organic thin film transistors and design of n-channel organic semiconductors. Chem Mater 2004;16:4436–51.
[18] Hwang IW, Xu QH, Soci C, Chen B, Jen AKY, Moses D, et al. Ultrafast spectroscopic study of photoinduced electron transfer in an oligo(thienylene-vinylene):fullerene composite. Adv Funct Mater 2007;17:563–8.
[19] Lee JY, Choi MH, Song HJ, Moon DK. Random copolymers based on 3-hexylthiophene and benzothiadiazole with induced π-conjugation length and enhanced open-circuit voltage property for organic photovoltaics. J Polym Sci A Polym Chem 2010;48:4875–83.
[20] Yasuda T, Imase T, Yamamoto T. Synthesis, characterization, and optical and electrochemical properties of new 2,1,3-benzoselenadiazole-based CT-type copolymers. Macromolecules 2005;38:7378–85.
[21] Yamamoto T, Lee BL, Kokubo H, Kishida H, Hirota K, Wakabayashi T, et al. Synthesis of a new thiophene/quinoxaline CT-type copolymer with high solubility and its basic optical properties. Macromol Rapid Commun 2003;24:440–3.
[22] Cheng YJ, Yang SH, Hsu CS. Synthesis of conjugated polymers for organic solar cell applications. Chem Rev 2009;109:5868–923.
[23] Kroon R, Lenes M, Hummelen JC, Blom PWM, de Boer B. Small bandgap polymers for organic solar cells (polymer material development in the last 5 years). Polym Rev 2008;48:531–82.
[24] Zhang M, Guo X, Zhang ZG, Li Y. D–A copolymers based on dithienosilole and phthalimide for photovoltaic materials. Polymer 2011. doi:10.1016/j.polymer.2011.10.007.
[25] Xin H, Guo X, Kim FS, Ren G, Watson MD, Jenekhe SA. Efficient solar cells based on a new phthalimide-based donor–acceptor copolymer semiconductor: morphology, charge-transport, and photovoltaic properties. J Mater Chem 2009;19:5303–10.
[26] Usta H, Risko C, Wang Z, Huang H, Deliomeroglu MK, Zhukhovitskiy A, et al. Design, synthesis, and characterization of ladder-type molecules and polymers. air-stable, solution-processable n-channel and ambipolar semiconductors for thin-film transistors via experiment and theory. J Am Chem Soc 2009;131:5586–608.
[27] Lee JY, Shin WS, Haw JR, Moon DK. Low band-gap polymers based on quinoxaline derivatives and fused thiophene as donor materials for high efficiency bulk-heterojunction photovoltaic cells. J Mater Chem 2009;19:4938–45.
[28] Gadisa A, Mammo W, Andersson LM, Admassie S, Zhang F, Andersson MR, et al. A new donor-acceptor-donor polyfluorene copolymer with balanced electron and hole mobility. Adv Funct Mater 2007;17:3836–42.
[29] Blouin N, Michaud A, Gendron D, Wakim S, Blair E, Neagu-Plesu R, et al. Toward a rational design of poly(2,7-carbazole) derivatives for solar cells. J Am Chem Soc 2008;130:732–42.
[30] Bundgaard E, Krebs FC. Low band gap polymers for organic photovoltaics. Sol Energy Mater Sol Cells 2007;91:954–85.
[31] Muhlbacher D, Scharber M, Morana M, Zhu Z, Waller D, Gaudiana R, et al. High photovoltaic performance of a low-bandgap polymer. Adv Mater 2006;18:2884–9.
[32] Reyes-Reyes M, Kim K, Carroll DL. High-efficiency photovoltaic devices based on annealed poly(3-hexylthiophene) and 1-(3-methoxycarbonyl)-propyl-1-phenyl-(6,6)C61 blends. Appl Phys Lett 2005;87:083506.
[33] Peet J, Kim JY, Coates NE, Ma WL, Moses D, Heeger AJ, et al. Efficiency enhancement in low-bandgap polymer solar cells by processing with alkane dithiols. Nature Mater 2007;6:497–500.